Vertical motions of the Puerto Rico Trench and Puerto Rico and their cause

Uri ten Brink
U.S. Geological Survey, Woods Hole, Massachusetts, USA

Received 30 September 2004; revised 19 January 2005; accepted 15 February 2005; published XX Month 2005.

[1] The Puerto Rico trench exhibits great water depth, an extremely low gravity anomaly, and a tilted carbonate platform between (reconstructed) elevations of +1300 m and −4000 m. I argue that these features are manifestations of large vertical movements of a segment of the Puerto Rico trench, its forearc, and the island of Puerto Rico that took place 3.3 m.y. ago over a time period as short as 14–40 kyr. I explain these vertical movements by a sudden increase in the slab's descent angle that caused the trench to subside and the island to rise. The increased dip could have been caused by shearing or even by a complete tear of the descending North American slab, although the exact nature of this deformation is unknown. The rapid (14–40 kyr) and uniform tilt along a 250 km long section of the trench is compatible with scales of mantle flow and plate bending. The proposed shear zone or tear is inferred from seismic, morphological, and gravity observations to start at the trench at 64.5°W and trend southwestwardly toward eastern Puerto Rico. The tensile stresses necessary to deform or tear the slab could have been generated by increased curvature of the trench following a counterclockwise rotation of the upper plate and by the subduction of a large seamount.

Citation: ten Brink, U. (2005), Vertical motions of the Puerto Rico Trench and Puerto Rico and their cause, *J. Geophys. Res.*, *110*, XXXXXX, doi:10.1029/2004JB003459.

1. Introduction

[2] Dynamic topography, that component of the topography, which is not isostatically, compensated, provides one of the few observations into the sublithospheric structure and processes in subduction zones [*Buiter et al.*, 2001; *Giunchi et al.*, 1996; *Zhong and Gurnis*, 1992, 1994]. For example, the extreme depth of oceanic trenches at subduction zone is thought to be in part due to slab pull forces. The Puerto Rico trench (PRT), with water depths of up to 8340 m, is the deepest part of the Atlantic Ocean, yet the relative plate motion along the PRT is predominantly strike slip with only a small component of North America (NOAM) plate subduction (N70°E [*Calais et al.*, 2002; *Mann et al.*, 2002]). The maximum slab depth under Puerto Rico and the Virgin Islands as revealed by earthquakes is only 150 km (Figure 1a), although the true depth extent of the slab has not been determined in tomographic studies. The gravity anomaly over trenches is another measure of their departure from isostatic equilibrium. Oceanic trenches are associated with very large negative free-air gravity anomalies. The PRT, despite being less deep than many Pacific Ocean trenches is associated with the most negative free-air gravity anomaly on earth, −380 mGal. The most negative anomaly is not located at the deepest point of the trench, but 50 km to the south, where the forearc is unusually deep, 7950 m (Figure 1b).

[3] Just how unusual these observations are can be appreciated by comparing the gravity and bathymetry of the PRT to other subduction zones. The South Sandwich subduction zone (Figure 2) is most often compared to the Antilles in its tectonic setting. The maximum water depth (∼7500 m) and minimum free-air gravity anomaly (∼−260 mGal) of the South Sandwich trench are located at the plate corner, whereas in the PRT, the deepest part is located west of the plate corner. A local gravity minimum at the curved northern end of the Tonga trench is associated with a local deep, but the deepest part of the trench and the lowest gravity anomaly are located farther south along the relatively straight segment of the trench (Figure 2). The Challenger Deep in the Mariana trough, the deepest place on Earth (∼11 km), resembles the PRT in some aspects, although its gravity anomaly is slightly less than that of the PRT. The trench outer slope is very steep and is highly faulted [*Fujioka et al.*, 2002]. The formation of the Challenger Deep was attributed to the passage and collision of the Caroline Ridge with the Mariana Trough [*Fujioka et al.*, 2002], to a tear in the subducting plate [*Fryer et al.*, 2003], or to a narrow coupling zone between the subducting and overriding plate [*Gvirtzman and Stern*, 2004].

[4] Many models, which cover almost the entire spectrum of tectonic processes, have been published during the past 40 years to explain the unusually deep water and the negative gravity anomaly in the PRT. However, these processes are incompatible with the observations below of the trench collapse, its geographical extent, and its timing

and duration. Here I propose a new hypothesis for the great water depth and the negative gravity anomaly of the PRT. I start by arguing that the anomalous bathymetry and gravity are due to the collapse of a segment of the trench relative to the adjacent trench segment, and I estimate the time and the duration of the collapse. I then propose that the collapse was caused by an abrupt increase in slab dip, perhaps following internal deformation or tearing of the slab NE of Puerto Rico. I point out that the collapse was accompanied by the rise of the island of Puerto Rico, which can also be explained by the increased slab dip. Finally, I analyze the forces that could have deformed the slab at this place. The paper ends with a discussion of alternative explanations for the collapse of the trench and the rise of the island.

2. Evidence for Trench Collapse

2.1. Bathymetry and Seismic Reflection

[5] The trench floor north and NE of the Virgin Islands (east of longitude 64.5°W) is 7000–7500 m deep, and is very narrow (Figure 1b), reflecting the paucity of sediment

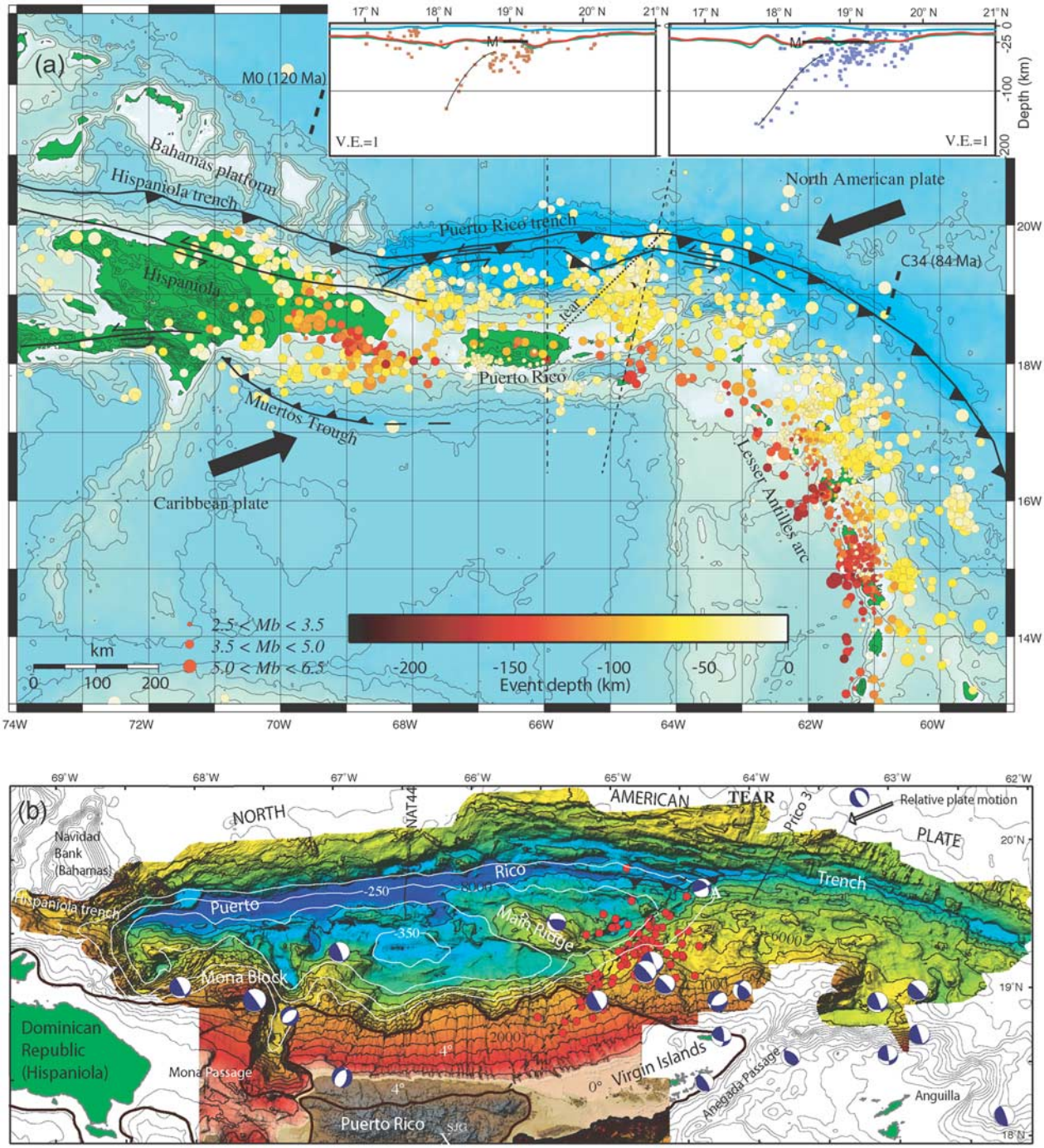

Figure 1

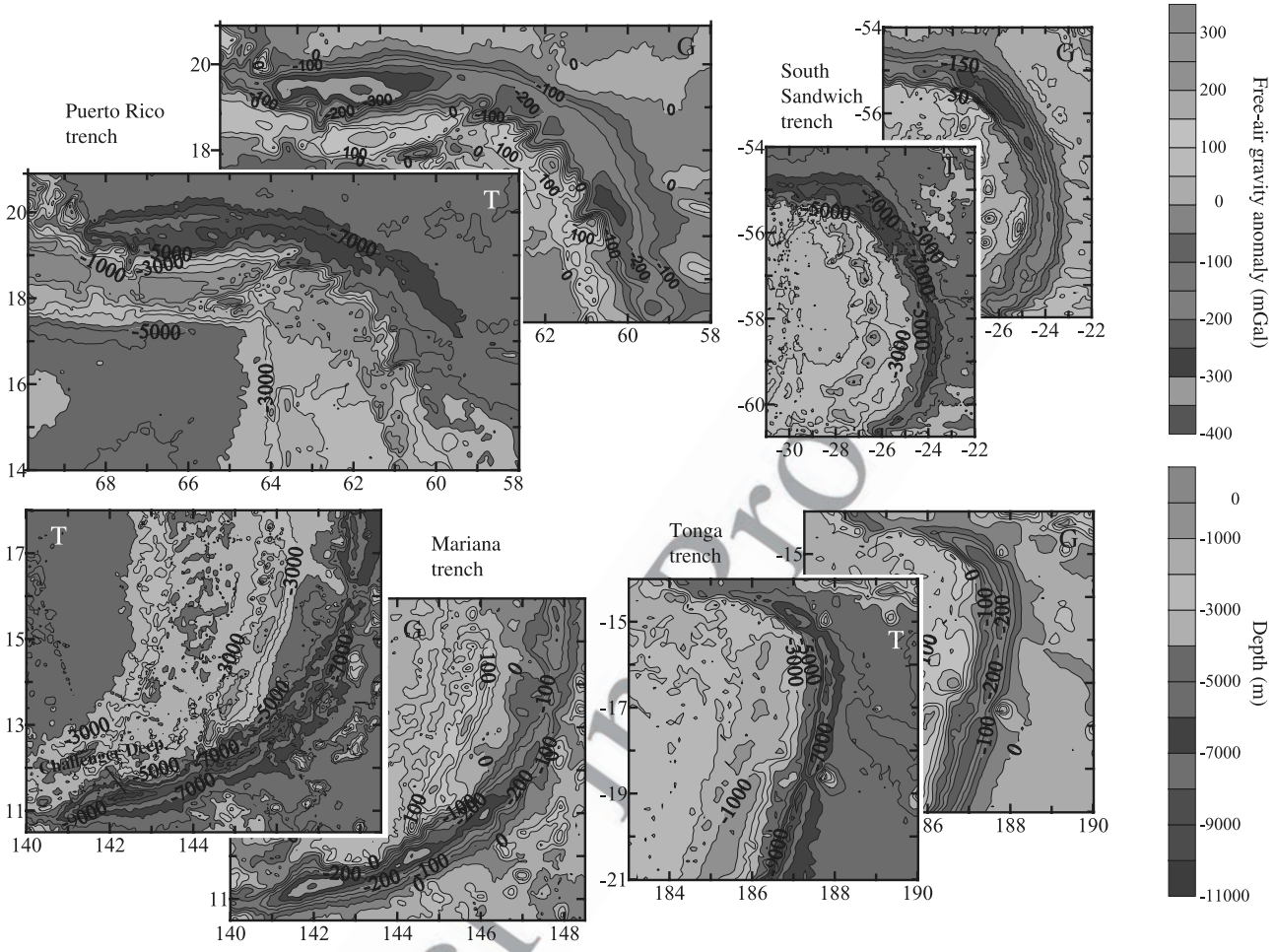

Figure 2. Free-air gravity G (in mGal) and bathymetry T (in m) [*Sandwell and Smith*, 1997; *Smith and Sandwell*, 1997] of several tightly curved subduction zones.

supply to the trench. The trench floor farther west between 65.3°–68.5°W is deeper (8340 m), wider, and flat. The forearc south of this collapsed section of the trench is also unusually deep, reaching 7950 m, compared with the much shallower forearc north of the Virgin Islands.

[6] Seismic profiles show that the deep, flat, and wide trench floor west of 64°W is underlain by normal-fault bounded blocks that appear to have rotated southward by collapse of the trench floor (Figure 3, NAT 44). In contrast, the fault bounded blocks under the narrow and shallower trench east of longitude 64.5° are not rotated, and descend in a "staircase" fashion under the overlying Caribbean plate (Figure 3, Prico 3).

[7] Puerto Rico and the Virgin Islands are situated on an older arc (Cretaceous to early Tertiary) that has been covered by a carbonate platform since the Late Oligocene [*Larue et al.*, 1998]. Although the carbonate platform was deposited horizontally close to sea level, it is presently tilted northward at approximately 4° and its northward edge reaches a depth of 4000 m [*Moussa et al.*, 1987]

Figure 1. (a) Seismicity from the relocated global earthquake database [*Engdahl et al.*, 1998] and the main tectonic features in the NE Caribbean region. Thick arrows are relative direction of plate convergence. Insets show cross sections of seismicity located within 111 km of the dashed lines in the main figure. Bathymetry (blue) and two estimates of the crust-mantle interface from two different 3-D inversions of the gravity field (red and green) (J.L. Martin and U.S. ten Brink, unpublished data) are also shown. Thick horizontal black lines are estimates of Moho depth from *Fischer and McCann* [1984] and *Brown and Gurrola* [2002]. (b) Shaded bathymetry of the northeast Caribbean and outline of the gravity anomaly (in mGal) over the PRT. Bathymetry contour interval is 0.5 km. Color bathymetry combines multibeam bathymetry at depths >2500 m, single-beam bathymetry at shallower depths, and lidar near shore (see *ten Brink et al.* [2004] for details). Dashed line is approximate location of proposed tear in the NOAM plate. Thin brown line is the extent of carbonate platform [*van Gestel et al.*, 1999]. Red dots show the subcrustal earthquake swarm during 16–22 October 2001, located by the Puerto Rico Seismic Network. Numbers with a degree symbol mark the tilt of the carbonate platform. Beach balls show earthquake focal mechanisms since 1976 from the Harvard CMT catalog. X is the location of the broadband seismic station SJG used for the receiver function analysis.

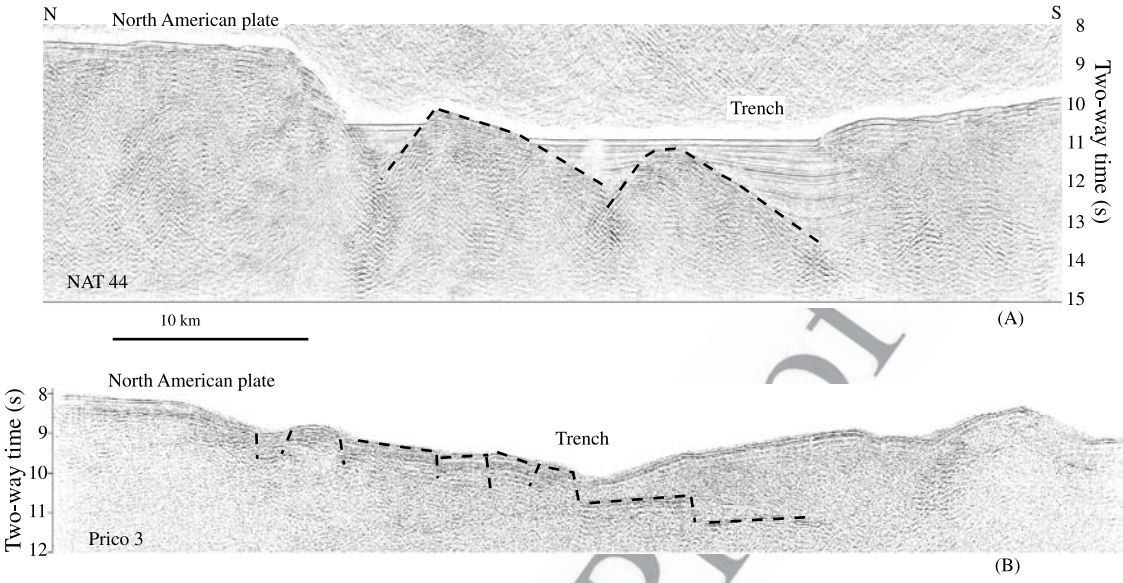

Figure 3. Comparison between geometry of the subducting NOAM plate along two migrated seismic profiles across the trench, (a) one within the collapsed trench region and (b) the other outside the region of collapse. See Figure 1b for location.

(Figure 1b). The dip of the carbonate platform is remarkably uniform along the 250 km long northern shelf of Puerto Rico and the U.S. Virgin Islands (Figure 4). To the south, the carbonate platform rises onshore in northern Puerto Rico, maintaining its constant undisturbed dip up to 20 km inland (Figure 1b), where it is completely eroded [*Zapp et al.*, 1948]. Were it not eroded, the platform top would have reached there an elevation of 1300 m above sea level. In contrast to Puerto Rico, the platform is flat at sea level around the Virgin Islands (Figure 1b).

2.2. Gravity

[8] The PRT is associated with the lowest free-air gravity anomaly on Earth. As expected, the shape of the free-air gravity anomaly mimics the bathymetry (Figure 1b). However, the lowest gravity anomaly is located over the forearc, where water depth is reaches 7950 m, and not over the trench itself, probably because the crust there is thicker than in the trench. The extremely negative anomaly (as defined by the −250 mGal contour) ends NE of Puerto Rico along a NW-SE orientation, across which the forearc bathymetry is significantly shallower.

[9] The residual gravity anomaly, which compensates for the variations in water depth, is also 40 mGal more negative in the area of the minimum free-air gravity anomaly than in the forearc farther east (Figure 5a). The residual gravity is the free air anomaly minus the contributions of the water layer and of a constant 7 km thick crust. It reflects variations in sediment thickness, crustal thickness, and mantle density. Sediment thickness in the PRT is relatively small, and mantle density variations are expected to produce longer wavelength anomalies. Therefore the negative residual gravity in the area of minimum free-air gravity anomaly probably reflects a thicker crust relative to the forearc farther east. 2-D gravity models along several seismic lines in the area (Figure 5) indicate that the lateral change in the residual gravity is indeed caused by variations in the crustal thickness of the forearc. In particular, models across the collapsed part of the trench (Figures 5c and 5d) show a steeper subduction interface near the trench and a thicker forearc crust than the model outside the anomaly (Figure 5b).

2.3. Earthquakes

[10] The shape of the slab at larger depths is generally outlined by earthquakes (the Wadati-Benioff zone). Although the number of earthquakes from the global relocated earthquakes data set [*Engdahl et al.*, 1998] is too small to map the slab dip in the NE Caribbean with certainty, the Wadati-Benioff zone appears to be steeper in the collapsed segment of the trench than in the to the east (Figure 1a, inset). Locally recorded earthquakes also appear to show a steeper slab north and northwest of Puerto Rico than northeast of Puerto Rico [*McCann*, 2002, Figure 4].

3. Timing and Duration of Trench Collapse

[11] The Pliocene Quebradillas Formation is the uppermost part of the carbonate section [*Moussa et al.*, 1987]. It is found both onshore and offshore Puerto Rico along almost the entire width of the island and, where not eroded, has a uniform thickness [*Moussa et al.*, 1987]). The lower part of the formation was deposited at water depths >200 m and the upper parts were deposited close to sea level [*Moussa et al.*, 1987]. The formation is separated from the underlying Oligocene-Miocene carbonate layers by an erosional unconformity that represents a hiatus in deposition during the time when the carbonate platform was slightly above sea level. [*Monroe*, 1980]. *Moussa et al.* [1987, p. 438] noted that "the dip of the Quebradillas is the same as that of the underlying units, both onshore and offshore, averages 4°, and is constant through the full length of the island". The monotonous tilt of the carbonate platform is

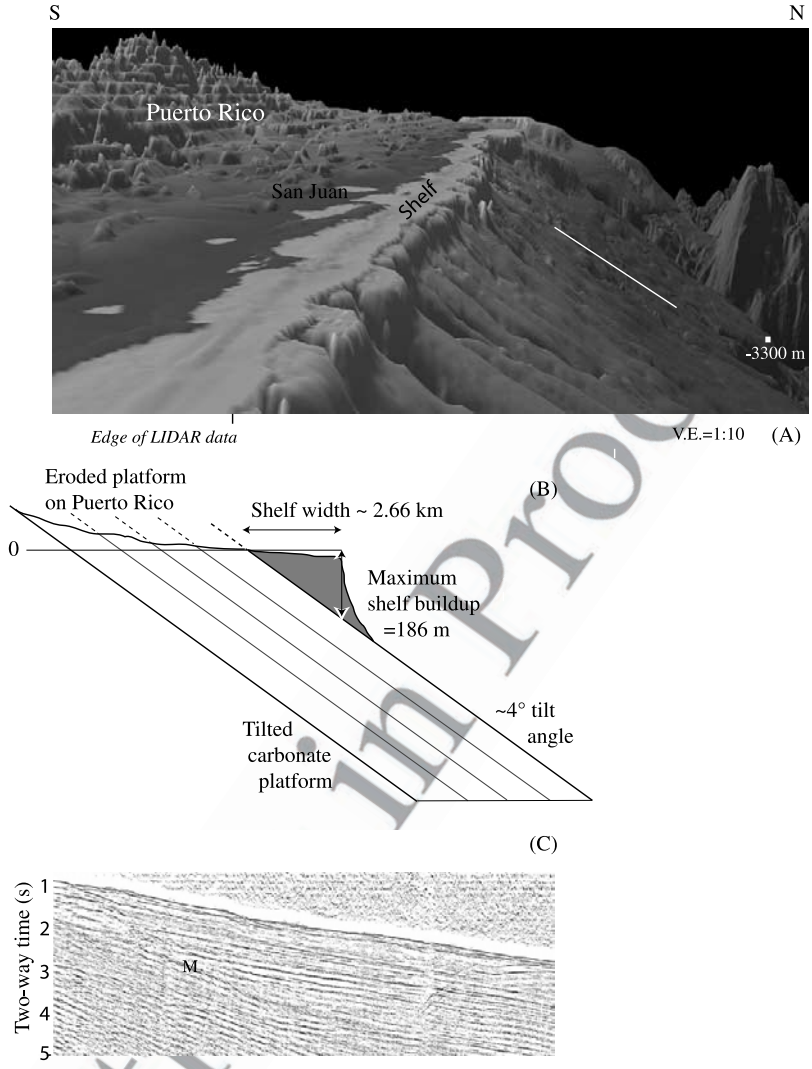

Figure 4. (a) Side view of the uniformly tilted carbonate platform and the narrow shelf north of Puerto Rico. White line is the location of the profile in Figure 4c. (b) Graphical representation of the method used to calculate the duration of the tilt event. (c) Section of migrated seismic profile NAT44 across the carbonate platform showing the uniform tilt of carbonate layers with depth. M is the water column multiple.

generally undisturbed by faults [*Meyerhoff et al.*, 1983; *Moussa et al.*, 1987; *Larue et al.*, 1998; *van Gestel et al.*, 1999] (Figure 4). A rapid tilting of the platform is inferred because no layers with lower dips have accumulated on top of the Oligocene-Pliocene carbonate platform. The only accumulation of post-Quebradillas rocks is the buildup of a narrow (<3 km wide) and shallow (0–100 m deep) shelf near shore (Figure 4a). Outcrops close to the coast record Plio-Pleistocene deposits, younger than 3.3 Ma [*Moussa et al.*, 1987]. I interpret the narrow shelf to be the only part of the margin where coral growth and carbonate precipitation kept pace with subsidence. Subsidence rate presumably increased linearly with distance seaward and was slow enough only in the vicinity of the shoreline near the hinge of the tilted platform to allow the shelf to grow (Figure 4b).

[12] If we know the thickness of the shelf edge, and the subsidence rate at the shelf edge, we can derive the duration of the tilting episode. The maximum subsidence rate at which shelf buildup could keep up with the tilting should be equal to the maximum growth rate of reefs or to the maximum sedimentation rate of carbonates. The maximum growth rate of *Acropora palmata*, a common shallow water coral in Puerto Rico and other Caribbean Islands, is 14 mm/y [*Buddemeier and Smith*, 1988]. The maximum sedimentation rate of carbonate platforms calculated over a time interval $\leq$10,000 years, is 5–11 mm/y [*Schlager*, 1998b]. The maximum carbonate production rate in back reefs and lagoons is 0.5 mm/y [*Bosence and Waltham*, 1990].

[13] The maximum thickness of the shelf is estimated as follows: The average width of the shelf north of Puerto Rico (Figure 4a), measured between the shoreline and the 100 m depth contour, is 2.66 km. The shelf edge does not appear to be eroded because the 100 m contour generally mimics the coastline (edge of light pink color in Figure 1b). With an average platform tilt angle of 4°, the shelf edge was built upward from a depth of 186 m (Figure 4b). Sea level in the

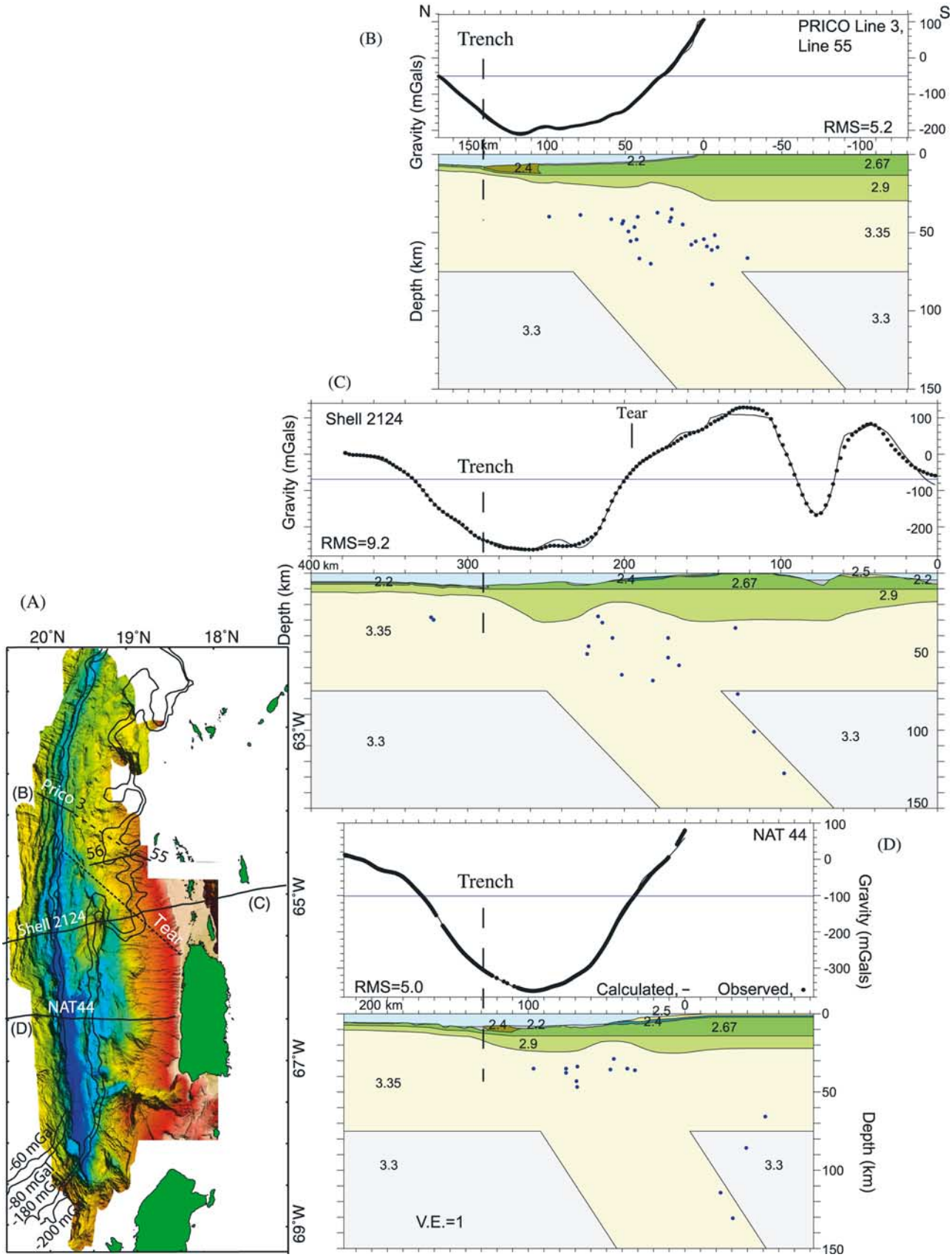
(A)
20°N
19°N
18°N
63°W
65°W
67°W
69°W
(B)
Prico 3
56
55
(C)
Shell 2124
Tear
(D)
NAT44
-60 mGal
-80 mGal
-180 mGal
-200 mGal
N
S
Trench
PRICO Line 3, Line 55
RMS=5.2
Gravity (mGals)
150 km
100
50
0
-50
-100
2.4
2.2
2.67
2.9
3.35
3.3
Depth (km)
Shell 2124
Tear
Trench
RMS=9.2
400 km
300
200
2.5
NAT 44
RMS=5.0
Calculated, –
Observed, •
200 km
V.E.=1

Figure 5

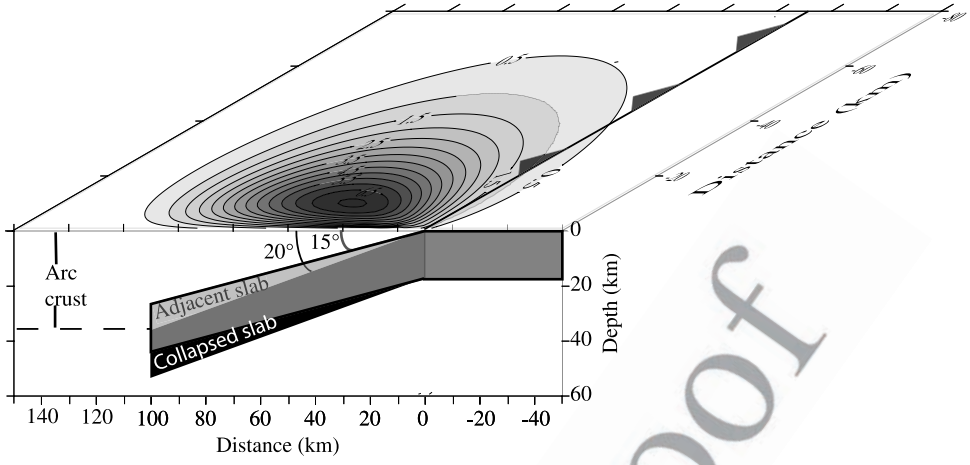

Figure 6. Predicted topography due to depth differences between adjacent slab segments having different dip angles. One slab dips at 15°, and the other dips at 20°. The offset between the slabs is modeled as a vertical fault with a throw proportional to the offset. The topography is modeled using 3-D elastic model (Coulomb 2.5 [*Toda and Stein*, 2002]), which can only handle infinitesimal strain, and therefore the modeled magnitude of the offset is 1% of the real offset. Modeling the offset as a vertical fault also results in the topographic depression diminishing with distance from the boundary between the segments, whereas in reality, the two segments remain in their respective depths along strike, and therefore the depression is expected to continue along strike.

Middle Pliocene was ~25 m above the present sea level [*Dowsett et al.*, 1999]. Therefore, at the northern edge of the narrow shelf, a reef had to grow (or carbonates had to be deposited) to a maximum of 211 m during the tilt event to catch up with the subsidence. However, *Acropora palmata* can grow in water as deep as 13–16 m [*Blanchon et al.*, 2002]. Therefore only corals that were no deeper than 13–16 m at the end of the tilting event could have continued to grow.

[14] We can now divide the shelf thickness at the shelf edge by its subsidence rate to find the duration of the tilt. If the subsidence rate equals the growth rate of the corals, then 198 m (211 m minus 13 m) divided by 14 mm/y gives the shortest time window of 14,140 years for the tilt event. (The duration will be even shorter if we choose 16 m as the limiting depth of coral growth). The longest time period for the tilt event is estimated as 198 m divided by the rate of carbonate sedimentation (5 mm/y), which yields 39,600 years to complete. However, if the carbonate sedimentation was the limiting rate for shelf growth, the thickness of the shelf edge at the end of the tilt event could have been smaller than 198 m, because maximum carbonate production takes place within 20 m of the surface and decreases to zero at 150 m water depth [*Schlager*, 1998a], and therefore the tilt duration would have been shorter than 39,600 years. Even if the published maximum rates of coral growth is off by an order of magnitude, or the shelf growth is limited by the rate of carbonate production (0.5 mm/y [*Bosence and Waltham*, 1990]), the estimated duration of the tilting, 0.15–0.4 Ma, had to be very rapid.

4. What Caused the Collapse of Part of the PRT and Forearc?

[15] I propose that a portion of the PRT and the forearc collapsed during a short time interval 3.3 m.y. ago because of a sudden increase in the dip angle of the slab interface there. The slab interface and the Benioff zone under Puerto Rico and the Virgin Islands cannot be mapped reliably to verify the change in slab dip because of the small number of large and moderate earthquakes. The available relocated earthquake data set, however, hints that this may be the case (Figure 1a, inset). The seismic lines (Figure 3) and gravity models (Figure 5) further suggest that the shallow subduction angle is steeper in the area of trench and forearc collapse, than in the area to the east. Published numerical models also predict that trench depth increases with increasing dip angle of the interface between the overriding and subducting plate, and with increasing slab dip angle [*Zhong and Gurnis*, 1994].

[16] The large difference in the depth of the forearc region between the collapsed and the normal segments is another

Figure 5. (a) Residual gravity anomaly along the PRT, location of proposed tear (dashed line), and location of gravity profiles in Figures 5b, 5c, and 5d. Residual gravity was calculated by subtracting the contribution of the water and a 7 km thick crust from the free-air gravity anomaly. (b–d) Observed (dots) and calculated (thin line) gravity profiles along reprocessed seismic profiles in the area. Seismic profiles constrain sediment thickness. Sediment thickness for the central part of the profile in Figure 5b was projected from a diagonal profile (line 56). Dark dots are subcrustal earthquake hypocenters from *Engdahl et al.*'s [1998] relocated global database.

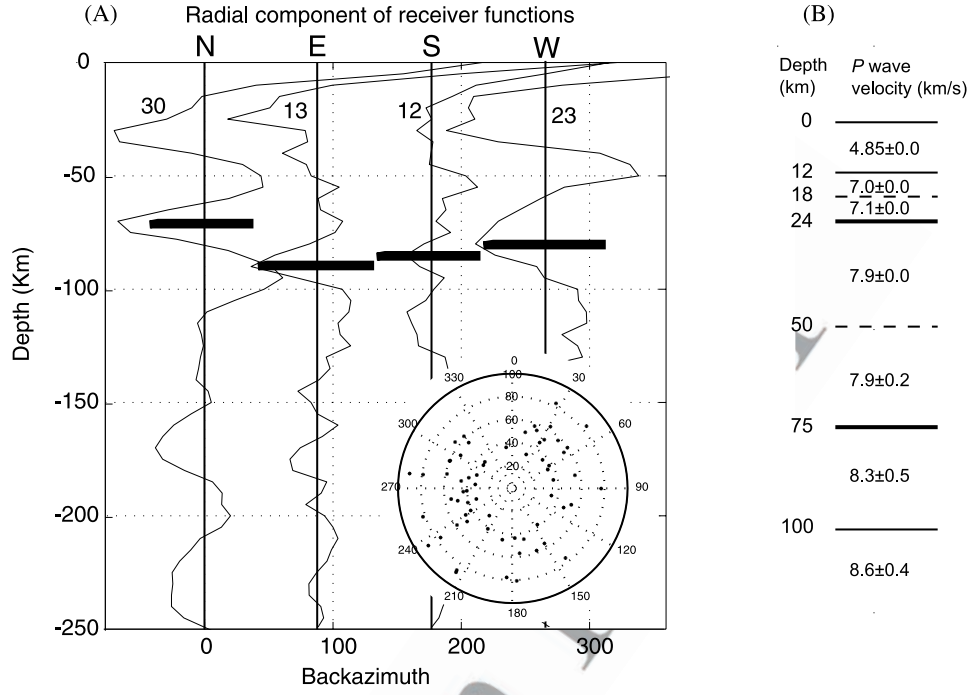

Figure 7. (a) Stacked radial component receiver functions computed from seismic data recorded at IRIS/USGS broadband seismic station SJG (see Figure 1b for location) between 1993 and 1999. Radial component receiver functions are computed by rotating the two horizontal component seismograms to isolate particle motion in the direction parallel to the great circle path from the earthquake to the seismic station and then deconvolving this signal by the vertical component of the seismogram. The vertical component is composed primarily of P wave energy for events arriving from the teleseismic distance range. The radial component therefore emphasizes S wave energy. The coda following the P wave is composed primarily of P-to-S converted energy. Hence, by deconvolving the vertical component, we recover amplitude coefficients and delay times for the P-to-S converted phases and reverberations from layers beneath the seismic station. The delay times for these arrivals were converted to depths (the vertical axis) using the IASPEI velocity model. The data were stacked into azimuthal bins 90° centered at 0° (north), 90° (east), 180°, and 270°. The number of arrivals being stacked is shown next to each trace. Stacking is necessary to draw weak Ps phase above noise levels and helps to minimize the effects of systematic scattering from 3-D structure. The arrival times for Ps phases from different distances were corrected for the time delays due to differences in ray path using a standard move out correction computed for the IASPEI velocity model. The circular diagram in the bottom right corner shows that both the azimuthal distribution and the distance range within every 90° azimuthal bin of events are well distributed. The large negative pulse marked by a bar on each of these traces is very likely a Ps converted phase from a layer with an inverted velocity gradient. At a depth of 75 km, teleseismic arrivals sample a ~30 km radius cone around the seismic station. (b) The 1-D velocity model beneath the Virgin Islands from inversion of P wave arrival times from local earthquakes [*Fischer and McCann*, 1984].

indication for the increase in dip angle of the slab interface. Figure 6 shows the predicted topographic effect of a change in dip angle from 15° to 20° between two adjacent slab segments. The effect is largest at distances of 10–50 km from the trench and diminishes thereafter, despite the fact that the difference between the depths to the upper surfaces of these segments continues to increase with distance from the trench. This is because the overlying plate acts as an elastic lid that distributes the offset between the two slab segments, and the thickness of this lid also increases with distance from the trench. The observed lateral depth differences between the collapsed segment and the normal segment to the east are indeed largest at distances <60 km, and can hardly be detected on the carbonate platform farther south.

5. Why Does the Island of Puerto Rico Exist?

[17] My reconstruction of the thickness of the carbonate layers at the southern edge of the carbonate platform, 20 km south of the northern shoreline of Puerto Rico, indicates that the island had been uplifted by at least 1300 m since the deposition of the last carbonate layer 3.3–3.6 Ma. In comparison, the carbonate layers surrounding the Virgin Islands are flat and near sea level. A seismic *P* wave velocity model for the Virgin Islands indicates a positive

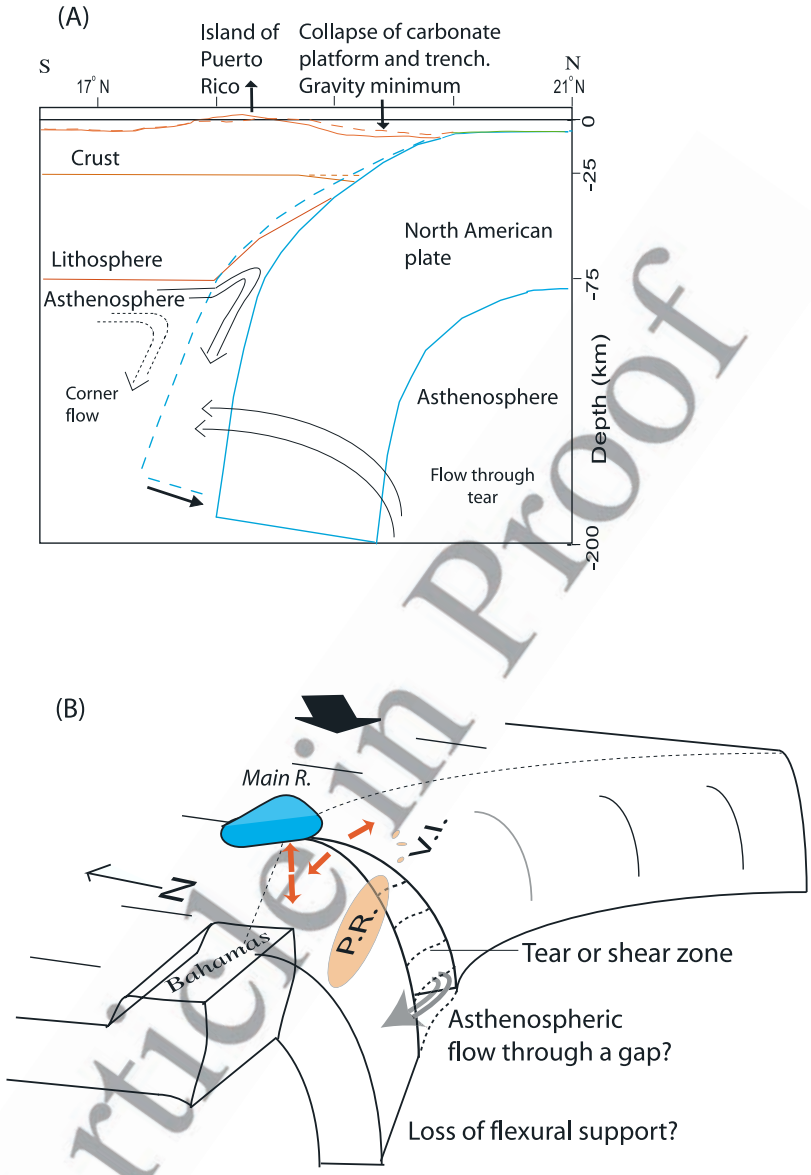

Figure 8. Sketches of the proposed model. (a) North-south cross section at the longitude of Puerto Rico showing the change in slab dip and topography from their initial profile (dashed lines) to their present profile (solid lines). Solid and dashed lines denote present an initial asthenospheric corner flow due to subduction. A flow from the underside of the subducting plate through a gap between the two segments through a gap between the two segments. (b) A 3-D view to the NE of the subducting North American oceanic plate and the thicker Bahamas crust beneath the NE corner of the Caribbean plate. The island Puerto Rico (P.R.) and the Virgin Islands (V.I.) are shown schematically. Orange arrows denote tensile stresses due to the curvature of the subducting slab and tensile stress due to the subduction of Main Ridge. Note the steeper dip of the slab under Puerto Rico relative to under the Virgin Islands. The nature of the boundary between the two slab segments is unknown and is represented here as a sharp cut for simplicity. Gray arrow shows a possible asthenospheric flow through a gap between the two slab segments from the underside of the subducting plate into the corner between the subducting and overlying plate. Thin dashed line is the PRT. Black arrow shows the relative direction of plate motion.

velocity step at a depth of 75 km, which was interpreted as the base of the lithosphere [*Fischer and McCann*, 1984] (Figure 7). On the other hand, receiver function analysis for a broadband seismic station in Puerto Rico (see station location in Figure 1b) shows reverse polarity at this depth (Figure 7), indicating a negative velocity step [*Brown and Gurrola*, 2002]. If this interpretation is correct, then the overriding lithosphere under the Virgin Islands is in direct contact with the descending NOAM slab, giving rise to a positive velocity step, whereas under Puerto Rico it is in contact with an asthenospheric wedge (Figure 8a), giving rise to a negative velocity step.

[18] Numerical models suggest that the shear stress imparted on the overriding plate by the descending plate

has a significant influence on the dynamic topography [*Cattin et al.*, 1997; *Zhong and Gurnis*, 1992]. The region above the interface becomes more depressed with increasing shear stress [*Cattin et al.*, 1997; *Zhong and Gurnis*, 1992], presumably because the gravitational pull of the slab is more efficiently transmitted to the upper plate. We attribute the existence of Puerto Rico as a single large island to the rebound that occurred when the dip angle of the interface increased and the lithosphere under Puerto Rico lost contact with the descending slab (Figure 8b). Without this rebound, Puerto Rico would probably have looked like the British and U.S. Virgin Islands, where the downgoing slab is still in contact with the overlying lithosphere (Figure 8a). Indeed, the rectilinear shape of Puerto Rico is not determined by faults along its north and south coasts. Instead, the finite rigidity of the overlying lithosphere dictates that the entire region south of the trench be tilted northward because of the collapse of the trench and the rebound under Puerto Rico. (The region west of Puerto Rico is submerged because of the present east-west crustal extension between Puerto Rico and Hispaniola, as will be discussed later).

6. Did Shearing or a Tear Cause an Increase in Subduction Angle?

[19] I suggest that the increase in slab dip and plate interface dip occurred because a shear zone or a tear developed in the downgoing slab and isolated a segment north of Puerto Rico from the much larger part of the slab to the east. This deformation zone could be sheared and extended or could be completely torn, and the rheology could vary from brittle at shallow depths to ductile at deeper depths. Present observations however, do not provide good constraints on the deformation style.

[20] If the slab segment of Puerto Rico had been held at a certain descent angle by the rigidity of the subducting NOAM slab under the Lesser Antilles arc, then a shear zone would have weakened this support causing it to sink (Figure 8a). The expected timescale for lithospheric bending is on the order of 10^5 years [*Watts*, 2001], in accord with the estimated duration of the tilt of the carbonate platform. Trench-perpendicular tears have been interpreted elsewhere (the northern end of the Tonga Trench [*Millen and Hamburger*, 1998] and the Kurile trench [*Tanioka et al.*, 1995]) by earthquake focal mechanisms, but the associated vertical motions near these tears are much smaller than in the PRT. This is perhaps because the slabs of northern Tonga and the Kurile trench are much deeper and much longer than the Puerto Rico segment, and are therefore supported by plate rigidity and by the surrounding mantle.

[21] The collapse of the PRT could also have been the result of a change in the balancing forces on the descending slab. The gravitational body force on the descending lithospheric plate acts to pull it vertically down. Counteracting this force is a lifting pressure or suction on the upper surface of the descending plate caused by an asthenospheric corner flow that is induced by the motion of the descending plate. The balance of these two forces is thought to keep the plate at a finite descent angle [*Stevenson and Turner*, 1977]. The suction force could be reduced, however, if the descending slab is narrow, allowing flow around the edges of the slab to partially relieve the suction force [*Dvorkin et al.*, 1993]. The short duration of the carbonate platform tilt, 15–40 kyr, is compatible with changes in asthenospheric flow, which have a timescale of 10^4–10^5 years.

[22] Finally, the westward increase in slab's age and the westward decrease in convergence rate might have contributed to the westward decrease in slab buoyancy once a shear zone or a tear developed. The oceanic lithosphere that enters the PRT is old, within the Cretaceous magnetic quiet zone (Figure 1a). A linear interpolation across the magnetic quiet zone gives an age of 99 Ma at the location of the tear and a westward increase age of 3.7 Ma/100 km. Plate convergence rate decreases from 14 mm/y at 62°W westward to 4.2 mm/y along the deepest part of the trench (Figure 1b). Correlations between seismic coupling and age and between seismic coupling and plate convergence rate were observed for individual subduction zones and are probably related to the decreasing buoyancy of the subducting plate with increasing age and with decreasing convergence rate [e.g., *Pacheco et al.*, 1993].

7. Where is the Shear Zone Located?

[23] The shear zone in the slab is inferred to originate next to the region of maximum deformation on the NOAM plate and at the place where the trench is locally deflected southward (barbed line in Figure 1b). Centroid moment tensor solution for one of the larger earthquakes in the swarm at 64.5°W (marked A in Figure 1b) shows left-lateral slip with a downdip component on a subvertical fault. It may reflect differential motion between a more steeply subducting part of the slab to the west, and the less steeply dipping part of the slab to the east. A similar focal mechanism was observed in a few earthquakes west of the northern edge of the Tonga trench [*Isacks et al.*, 1969] and along the south edge of Carnegie Ridge [*Gutscher et al.*, 1999] and was interpreted to indicate tearing of the subducting Pacific and Nazca plates there, respectively. Tear earthquakes are expected to occur even after a shear or a tear has been established, because the tear continues to propagate into the plate entering the trench.

[24] The proposed location of the shear zone or the tear (dashed line marked "Tear" in Figure 1b) is coincident with the trend of the 16–22 October 2001 subcrustal earthquake swarm. The swarm consisted of 80 earthquakes having magnitudes $M_L < 5.5$ at subcrustal depths (Figure 1b). The larger seismic events were felt along the north shore of Puerto Rico but not in the Virgin Islands, which are closer to the epicenter (C. von Hillebrandt, personal communication, 2001). The proposed tear or shear zone location is also coincident with the eastern edge of the free-air gravity anomaly, the edge of the residual gravity anomaly, and the change in forearc depth. It may continue farther south to the NE corner of the island of Puerto Rico, which separates the uplifted and tilted carbonate platform onshore Puerto Rico from the flat and submerged carbonate platform around Culebra, Vieques, and the Virgin Islands. There is no surface

faulting in the forearc or the arc along this entire trend, which argues that the deformation is subcrustal.

8. What Might Have Caused the Deformation?

8.1. Tensile Stresses due to Trench Curvature

[25] One source of lateral stresses within the descending plate is its curvature in plan view (Figure 8b). *Frank* [1968] noted that the arcuate shape of trenches is a geometrical consequence of subduction of thin spherical shells and suggested that the surface area of an inextensible plate is conserved only if the radius of the curvature of the arc equals twice the dip of the subducting plate. Focal mechanisms of earthquakes indicating lateral tensile stresses within the descending plate were observed in some arcs with radius of curvature less than twice the subduction dip [*Burbach and Frohlich*, 1986].

[26] Paleomagnetic results of the carbonate layers indicate that Puerto Rico underwent 22 ± 9° of counterclockwise rotation after 11 Ma and that the rotation was complete by 4.5 Ma [*Reid et al.*, 1991]. This rotation could have increased the trench curvature, and consequently the plan view curvature of the NOAM plate (Figure 9). By 11 Ma, the PRVI block had cleared the Bahamas platform, except perhaps for the NW corner of the PRVI block, which was still pinned down by the SE tip of the Bahamas. This may have caused the PRVI block to rotate CCW. The consequences of this rotation might include the opening of the Yuma and Cabo Rojo rifts (Figure 9) and the termination of Caribbean underthrusting south of Puerto Rico. The rotation also resulted in an oblique left lateral opening of Anegada Passage, which is corroborated by observations [*Gill et al.*, 1999], because the Caribbean plate was moving eastward at a faster rate than the rotated PRVI block. By 4.5 Ma, the PRVI block was aligned with the Caribbean plate [*Reid et al.*, 1991] and, according to GPS results, is presently moving at the same rate and direction (within measurement errors) relative to NOAM as the Caribbean plate [*Calais et al.*, 2002; *Jansma et al.*, 2000; *Mann et al.*, 2002]. The movement of Hispaniola, however, continues to be impeded by the Bahamas [*Calais et al.*, 2002; *Jansma et al.*, 2000; *Mann et al.*, 2002; *Vogt et al.*, 1976] producing collision and mountain building in western Hispaniola, subduction of the Caribbean plate under eastern Hispaniola, and opening of the Mona Passage (Figure 1b).

[27] As the trench curvature increased, the obliquely descending NOAM plate was subjected to increasing lateral strain. In Figure 9 the trench-parallel extensional strain is calculated after rotation at a distance of 90 km from the trench along the trajectory and plane of the descending plate, which corresponds to a depth of 30 km assuming an average orthogonal descent angle of 20°. The calculated lateral strain shows an increase in the vicinity of the proposed tear after the rotation took place (Figure 9). However, tensile stresses due to increased curvature of the subducting plate are by themselves probably insufficient to tear the plate, because such tears are not observed in other tightly curved trenches such as the South Sandwich (Figure 2) and the Hebrides.

8.2. Tensile Stresses due to Seamount Subduction

[28] Subduction of seamounts and aseismic ridges is known to disrupt the subduction process [e.g., *Gutscher et al.*, 1999]. I propose that the underthrusting of Main Ridge (Figure 10a), a 50–60 km long and about 2000 m high ridge, was the immediate cause of the tear in the descending NOAM plate. The highest peak of Main Ridge, when projected 3.3 m.y. ago in the direction and rate of relative plate convergence (N70°E at 20 mm/y) was located at the shear zone or the tear close to the southward deflection of the trench axis at long 64.5°W (Figure 10).

[29] Following *McCann and Sykes* [1984], I interpret Main Ridge to be a subducted volcanic ridge (an aseismic ridge) because its axis is subperpendicular to the observed abyssal hill grain of the subducting NOAM plate north of the trench between 62°W and 66°W (Figure 1b). A focal mechanism of an earthquake from this location indicates active compression (Figure 10a). A comparison of tectonic features in the vicinity of Main Ridge with features predicted by sandbox models of subducting seamounts (Figure 10b) supports the interpretation of Main Ridge as a subducting seamount. Sandbox models predict the development of a frontal thrust and a back thrust on either side of the seamount [*Dominguez et al.*, 2000]. A reentrant in the forearc is expected to develop where the seamount entered the trench, and strike-slip faults bound the sides of the seamount trajectory in the forearc [*Dominguez et al.*, 2000]. These predicted features are observed in the PRT and forearc (Figure 10a). The southward deflection in the trench is interpreted to be the reentrant that was formed in the wake of the seamount subduction (Figure 10a). Because subduction is highly oblique, only one strike slip fault formed parallel to the trajectory of Main ridge. A seismic profile through the frontal thrust and back thrust faults show that they are juvenile, deflecting and pulling up sediments that were laid horizontally (Figure 10c).

[30] A subducting seamount sticks above the interface between the plates and is therefore expected to generate additional resistance to subduction. Resistance to subduction is transmitted within the subducting slab and in the overlying plate in the form of in-line stresses. These stresses were modeled as static stress changes using Coulomb 2.5 Program [*Toda and Stein*, 2002] as follows. The resistance to subduction on a limited patch of the interface was modeled by imposing displacement on this patch in a direction opposite to the subduction direction, and no motion in the surrounding interface. Stress changes arising from this displacement were calculated on fault planes dipping at 60° down slab. The calculations shows large tensile stresses developing within the slab downdip of the seamount and under its frontal part (Figures 10d and 10e). This stress change pattern appears to be corroborated by observations in the Hikurangi subduction zone, New Zealand. A normal fault that cuts through the upper part of the slab there was associated with a sequence of earthquakes with normal mechanisms that were located along a plane dipping 60° down slab [*Robinson*, 1994]. The fault was located beneath the frontal part of a 20 km wide ramp on the slab interface [*Louie et al.*, 2002].

[31] The calculated stress changes (Figures 10d and 10e) indicate that the subduction of Main Ridge 3.3 m.y. ago could have induced extension within the NOAM slab. Since Main Ridge was subducted in a direction that is subparallel to the trench, the extension direction is expected to have been subparallel to the trench. This may have triggered the

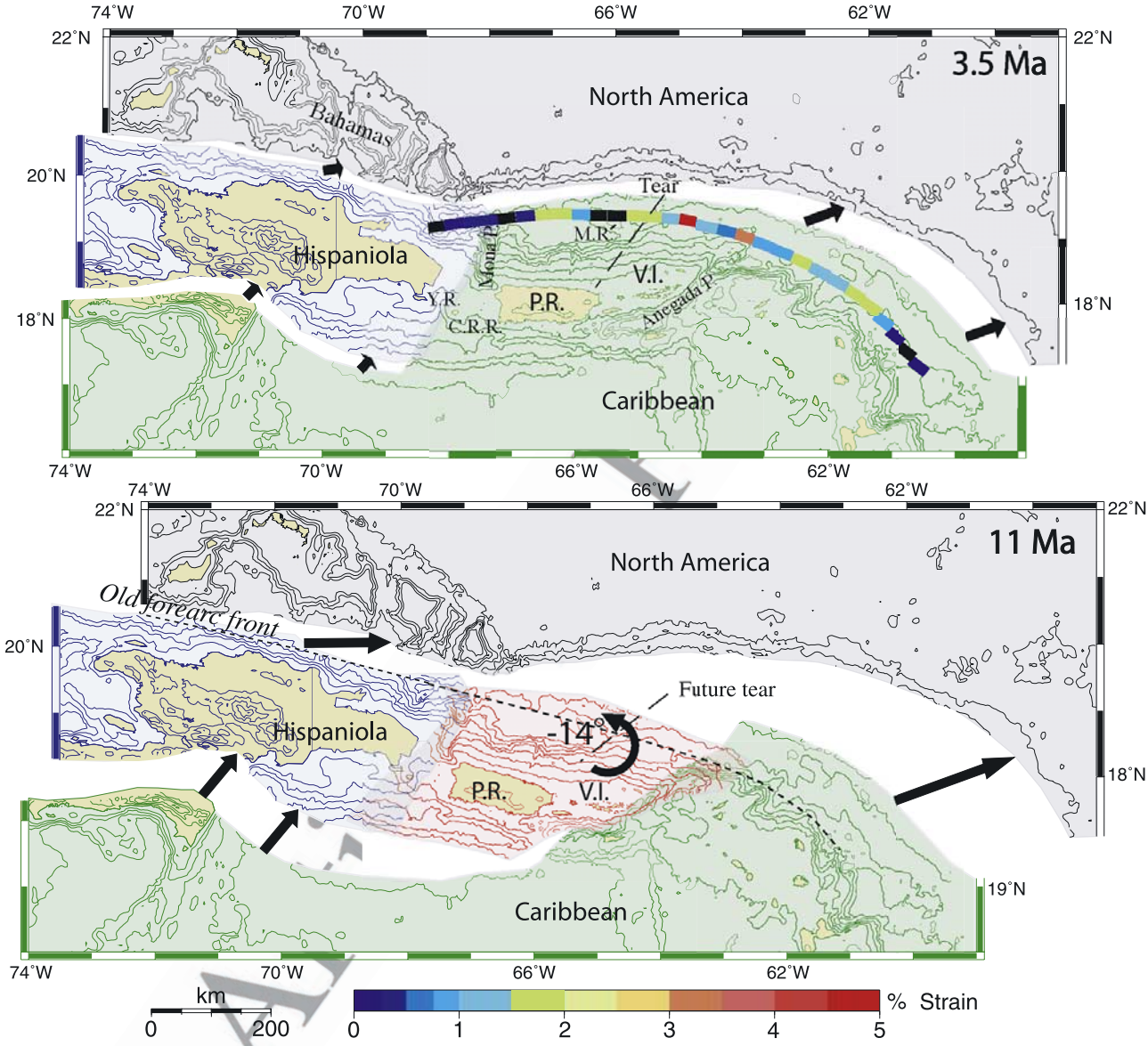

Figure 9. Kinematic reconstruction of the NE Caribbean (a) before the rotation of the Puerto Rico and Virgin Islands (P.R. V.I.) block 11 Ma [*Reid et al.*, 1991] and (b) after rotation ended but before the collapse of the carbonate platform 3.5 Ma. It is assumed that at 11 Ma the arc (dashed line) was continuous from the Lesser Antilles to Hispaniola and that the Caribbean plate has moved since then at a an average rate of 20 mm yr^{-1} in a direction 70° relative to North America (black arrows). Areas of overlap in the 11 Ma panel result in later rifting such as in the Mona, Yuma (Y.R.), and Cabo Rojo rifts (C.R.R.) and in the Anegada Passage. White regions are regions of later shortening by subduction or collision. The assumed 14° rotation in our reconstruction is within the error in the paleomagnetic results (J. Reid, personal communication, 2001) and minimizes the amounts of extension and shortening along the block boundaries. Multicolored line is the calculated lateral strain within the descending plate caused by its subduction under the curved PRT. Strain was calculated by comparing the distance intervals along the trench axis to distance intervals of their trajectories along the subduction direction (250°) 90 km away. The trajectories are plotted at their surface projection. Average plate descent angle perpendicular to the trench is 20°. Comparison between curvatures of the 11 Ma and 3.5 Ma (as represented by the forearc front) shows increased strain with trench curvature due to block rotation. Dashed line is the future location of the tear.

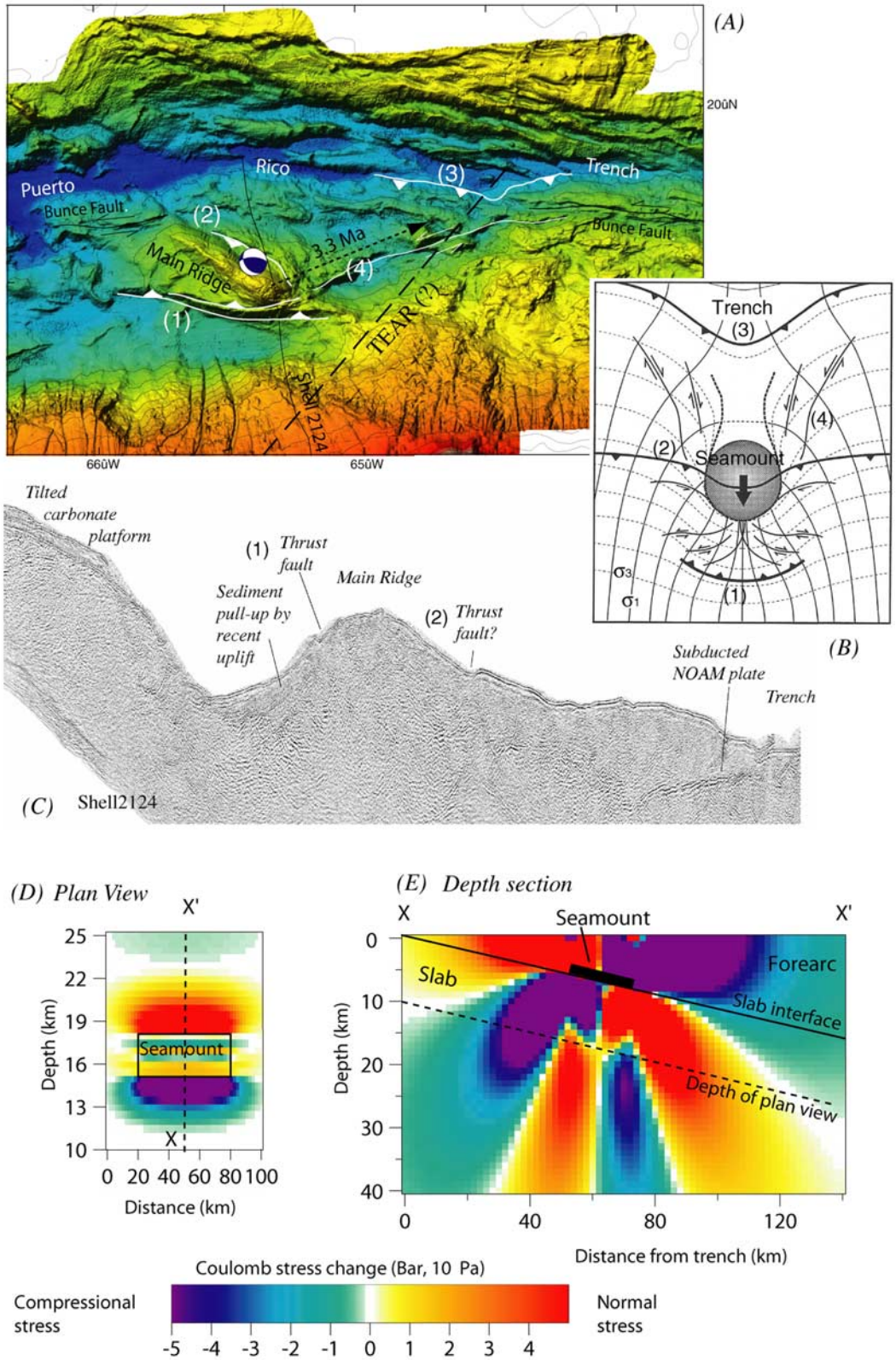
(A)
20ûN
Puerto Rico
Bunce Fault
(1)
(2)
(3)
(4)
Main Ridge
3.3 Ma
TEAR (?)
Trench
Bunce Fault
Shell 2124
66ûW
65ûW
Trench
(3)
(4)
(2)
Seamount
σ3
σ1
(1)
(B)
Tilted carbonate platform
(1) Thrust fault
Main Ridge
Sediment pull-up by recent uplift
(2) Thrust fault?
Subducted NOAM plate
Trench
(C) Shell2124
(D) Plan View
X'
X
Seamount
Depth (km)
Distance (km)
(E) Depth section
X
X'
Seamount
Slab
Forearc
Slab interface
Depth of plan view
Depth (km)
Distance from trench (km)
Coulomb stress change (Bar, 10 Pa)
Compressional stress
Normal stress

Figure 10

deformation in an area already subjected to trench-parallel tensile stresses due to the trench curvature (Figure 8).

9. Alternative Models

[32] The vertical motions described in this paper are attributed to a sudden increase of slab dip in part of the Puerto Rico trench, due to intraslab shearing, extension, or perhaps a complete tear. Next I discuss alternative models to explain these observations.

9.1. Subduction Initiation

[33] Quantitative models of subduction initiation at fracture zones [*Hall et al.*, 2003] and qualitative models of spontaneous subduction [*Stern*, 2004] predict rapid subsidence of the trench and forearc. Subsidence of the Puerto Rico trench and forearc could be interpreted in this context as a change from a transform plate boundary to subduction about 3.3 Ma. There are, however, several difficulties with this interpretation. The subduction initiation models predict a rapid roll back of the subducting plate that is associated with reheating and extension of the forearc and MORB-like volcanism, but there is no indication of reheating and volcanism in the forearc. *Observations* from New Zealand [*Stern and Holt*, 1994] indicate broad platform subsidence of the back arc region at the onset of subduction, which is not observed in the Caribbean plate. *Hall et al.* [2003] model predicts a very short uplift phase of the arc followed by 1–2 km of subsidence, contrary to the observed uplift of Puerto Rico. Other models [*Toth and Gurnis*, 1998] and observations from New Zealand [*House et al.*, 2002] suggest, however, several kilometers of dynamic uplift during the incipient subduction.

[34] The geologic history of the northern Caribbean plate boundary also argues against the interpretation of vertical motions as arising from subduction initiation. Cretaceous to early Tertiary subduction took place under Puerto Rico and the Virgin Islands, which are made of volcanic arc rocks. The youngest plutonic rocks are 45 Ma in Puerto Rico and 35 Ma in the Virgin Islands [e.g., *Larue et al.*, 1998]. The geometry of Cayman Trough along the NOAM/Caribbean plate boundary farther west [e.g., *ten Brink et al.*, 2002, and references therein] indicates a stable (within a few degrees) direction and rate (within 5 mm/y) of relative plate motion since 49 Ma. Therefore it is difficult to envision in this context how only a segment of the plate boundary will change from a transform plate boundary to subduction initiation.

9.2. Interaction of Two Subducting Slabs

[35] *Dillon et al.* [1996] proposed that downward pressure of the subducted edge of the Caribbean plate on the subducted edge of the NOAM plate under Puerto Rico and the Virgin Islands caused the latter to deepen. *Dolan et al.* [1998] pointed out subduction of the Caribbean plate may only take place under the Dominican Republic, and not under Puerto Rico. GPS results [e.g., *Jansma et al.*, 2000; *Mann et al.*, 2002] show the motion of Puerto Rico and the Virgin Islands to be similar (within measurement error) to that of the Caribbean plate. Moreover, the seismic activity south of Puerto Rico is sparse (Figure 1b) and does not indicate subduction of the Caribbean plate there. In addition, the rate of NOAM slab deepening by this process is expected to be slow contrary to the deduced rate of the carbonate platform collapse and its abrupt initiation.

9.3. Subduction Erosion

[36] Erosion of the base of the forearc by NW-SE oriented topographic ridges on the subducting NOAM plate was suggested to be the cause for the large depth of the Puerto Rico trench and the collapse of the carbonate platform [e.g., *Birch*, 1986]. These proposed ridges included Main Ridge [*McCann and Sykes*, 1984], two "fracture zones" (Main Ridge and a parallel ridge 100 km to its west [*Muszala et al.*, 1999]), and Mona Block (Figure 1b, 19.1°N, 67.7°W) [*Mann et al.*, 2002]. However, the observations do not support this interpretation. First, tectonic erosion of a narrow ridge would not have generated a large negative gravity anomaly, or the unusually deep and uniform trench floor along a 250 km long section of the trench (Figure 1b). Second, the fastest known forearc subsidence attributed to subduction erosion is at the Tonga Trench at 26°S (>2 km in 3 m.y.) [*Clift and Vannucchi*, 2004], much slower than the rate deduced here. Because of the relative plate motion, the various proposed ridges should have swept under the trench and forearc from east to west along a N70°W trajectory at a rate of 20 km/m.y. It would have therefore taken Mona Block 17.5 m.y. to traverse the subsided area west of 64.5°W (Figure 1b), and Main Ridge and the fracture zone to its west would not have traversed yet the entire area. The slow traverse would have resulted in a differential subsidence starting in the east and extending slowly to the west and in a slow differential tilt of the carbonate platform that should be manifested by increasing layer dip with depth. Neither one is observed.

Figure 10. (a) Enlargement of the bathymetry in the vicinity of the tear and Main Ridge showing several features that are predicted by sandbox models of forearc deformation due to the subduction of a seamount. (1), frontal thrust; (2), back thrust; (3), reentrant; (4), strike-slip fault along trajectory of seamount subduction. Arrow shows location of Main Ridge 3.3 m.y. ago, assuming relative plate motion of 20 mm yr^{-1} at azimuth N70°E. (b) Interpretation of sandbox model results of a subducted seamount from *Dominguez et al.* [2000]. (c) Part of reprocessed seismic profile shell 2124 showing thrust faults with opposing dips around Main Ridge. (d and e) Coulomb stress changes due to the subduction of a seamount. A seamount is expected to resist subduction more than a smooth slab interface. The resistance of the seamount to subduction was modeled using Coulomb 2.5 [*Toda and Stein*, 2002] by imposing displacement on a 20 × 60 km wide patch on the slab interface in a direction opposite to the subduction direction and by assuming no motion in the surrounding interface. The stresses were calculated on fault planes dipping at 60° down slab. Plan view of the stresses calculated at a depth of 10 km (dashed line on the depth section) is shown in Figure 10d. Depth section along the center of the seamount (dashed line on the plan view) is shown in Figure 10e. Positive indicates increased normal stress, and negative indicates increased compressive stress.

9.4. Crustal Forces

[37] Published crustal models to explain the unusual observation of the Puerto Rico trench cover almost the entire spectrum of tectonic processes. These models included transtension and rifting at the trench [*Bunce and Fahlquist*, 1962; *Speed and Larue*, 1991], N-S compression and buckling [*van Gestel et al.*, 1998], subsidence and uplift due to geometrical complications in a strike-slip fault system [*Jany et al.*, 1990], and subsidence and uplift due to counterclockwise rotation of the Puerto Rico/Virgin Island (PRVI) block [*Masson and Scanlon*, 1991]. Crustal forces that operate by repeated fault ruptures will result in a slower deformation rate than mantle flow, thus it will be difficult to explain the short duration of subsidence (tens to hundreds of kiloyears) by crustal extension, block rotation, or crustal compression. In addition, there is little evidence of large active crustal faults that accommodate brittle deformation within the forearc, as suggested by these models (e.g., Figure 1b). Moreover, brittle deformation is unlikely to create a uniform tilt angle along a 250 km long section of the plate boundary. Finally, models such as compression and buckling are not likely to generate the amplitude of negative gravity anomaly that is observed over the trench and forearc.

10. Summary and Conclusions

[38] The hypothesis described here offers a coherent explanation to many observations in the NE Caribbean, which puzzled scientists for the past 40 years. These observations include the unusually great depth of part of the PRT, the lowest free-air gravity anomaly on Earth, and a tilted Oligo-Pliocene carbonate platform whose northern edge is at a depth of 4000 m bsl and whose reconstructed southern depth is at an elevation of 1300 m asl. The platform is uniformly tilted along a 250 km long section of the trench, and the duration of the tilting event is estimated at between 15–40 kyr. I propose that these large vertical movements were generated in the middle Pliocene, when the dip of a segment of the descending NOAM slab was suddenly increased. The increased descent angle would have caused the trench and the proximal forearc to subside. It would also have caused the upper plate under the arc to detach from the descending slab. This would have allowed the arc to rise, which created the island of Puerto Rico.

[39] The increasing slab dip is attributed to deformation within the slab that caused it to shear, extend, and perhaps even tear. The increased slab dip could have been caused by either the loss of the ''suction force'', which balances the gravitational pull on the slab due to sideways asthenospheric flow through the tear, or because this segment lost the support of the rest of the descending rigid slab. On the basis of gravity, topography, seismic activity, focal mechanisms, and deformation of the seafloor, we locate the tear or the shear zone along a diagonal trend extending from the trench north of the Virgin Islands southwestward toward the northeastern edge of Puerto Rico.

[40] Two processes might have caused the slab to tear 3.3 m.y. ago. Counterclockwise rotation of the PRVI block during the Late Miocene probably increased the trench curvature, which would have increased the trench-parallel tensile stresses in the slab. Into this tighter curvature entered a large seamount about 3.3 m.y. ago, which would have created additional tensile stresses within the slab beneath the seamount.

[41] The model proposed here provides a tectonic framework for the NE Caribbean plate boundary, which will help in the assessment of earthquake and tsunami hazards for Puerto Rico, and the British and U.S. Virgin Islands [*ten Brink et al.*, 1999]. Beyond the regional interest, it shows that geological phenomena of the scale observed here can arise from local crustal interactions through coupling between lithosphere and asthenosphere and between horizontal and vertical tectonic forces. Finally, the contrast between the collapsed trench and uplifted island in the Puerto Rico section of the subduction zone, and the adjacent more normal subduction zone of the Virgin Islands, provides constraints on dynamic models of subduction zones. A more detailed study of the history of the collapse of the carbonate platform may help constrain the rheological properties of the slab and its surrounding asthenosphere, and may also provide constraints on rates of reef and platform growth during sea level rise.

[42] **Acknowledgments.** I thank Harold Gurrola for providing Figure 7 and Victor Huerfano for the locations of the 2001 earthquake swarm. Discussions with Bill Dillon, Dan Muhs, Bill McCann, Jian Lin, Roger Buck, and Robert Stern are gratefully acknowledged. Jennifer Martin, Jianli Song, Pilar Llanes Estrada, and Brian Andrews assisted with the modeling and with graphics. I thank Jian Lin, Stephanie Ross, Bill Dillon, Roberto Sabadini, and anonymous Associate Editor and reviewer for their constructive comments.

References

Birch, F. S. (1986), Isostatic, thermal, and flexural models of the subsidence of the north coast of Puerto Rico, *Geology*, *14*, 427–429.

Blanchon, P., B. Jones, and D. C. Ford (2002), Discovery of a submerged relic reef and shoreline off Grand Cayman; further support for an early Holocene jump in sea level, *Sediment. Geology*, *147*, 253–270.

Bosence, D., and D. Waltham (1990), Computer modeling the internal architecture of carbonate platforms, *Geology*, *18*, 26–30.

Brown, S., and H. Gurrola (2002), Receiver function analysis of the crust and upper mantle beneath Puerto Rico, *Eos Trans. AGU*, *83*(46), Fall Meet. Suppl., F957.

Buddemeier, R. W., and S. V. Smith (1988), Coral reef growth in an era of rapidly rising sea level: Predictions and suggestions for long-term research, *Coral Reefs*, *7*, 51–56.

Buiter, S. J. H., R. Govers, and M. J. R. Wortel (2001), A modelling study of vertical surface displacements at convergent plate margins, *Geophys. J. Int.*, *147*, 415–427.

Bunce, E. T., and D. A. Fahlquist (1962), Geophysical investigation of the Puerto Rico trench and outer ridge, *J. Geophys. Res.*, *67*, 3955–3972.

Burbach, G. V., and C. Frohlich (1986), Intermediate and deep seismicity and lateral structure of subducted lithosphere in the circum-Pacific region, *Rev. Geophys.*, *24*, 833–874.

Calais, E., Y. Mazabraud, B. Mercier de Lepinay, P. Mann, G. S. Mattioli, and P. E. Jansma (2002), Strain partitioning and fault slip rates in the northeastern Caribbean from GPS measurements, *Geophys. Res. Lett.*, *29*(18), 1856, doi:10.1029/2002GL015397.

Cattin, R., H. Lyon-Caen, and J. Chery (1997), Quantification of interplate coupling subduction zones and forearc topography, *Geophys. Res. Lett.*, *24*, 1563–1566.

Clift, P. D., and P. Vannucchi (2004), Controls on tectonic accretion versus erosion in subduction zones: Implications for the origin and recycling of the continental crust, *Rev. Geophys.*, *42*, RG2001, doi:10.1029/2003RG000127.

Dillon, W. P., N. T. Edgar, K. M. Scanlon, and D. F. Coleman (1996), A review of the tectonic problems of the strike-slip northern boundary of the Caribbean Plate and examination by GLORIA, in *Geology of the United States' Seafloor: The View From GLORIA*, edited by J. V. Gardner, M. E. Field, and D. C. Twichell, pp. 135–164, Cambridge Univ. Press, New York.

Dolan, J. F., H. T. Mullins, and D. J. Wald (1998), Active tectonics of the north-central Caribbean: Oblique collision, strain partitioning, and opposing subducted slabs, *Spec. Pap. Geol. Soc. Am.*, *326*, 1–62.

Dominguez, S., J. Malavieille, and S. E. Lallemand (2000), Deformation of accretionary wedges in response to seamount subduction: Insights from sandbox experiments, *Tectonics*, *19*, 182–196.

Dowsett, H. J., J. A. Barron, R. Z. Poore, R. S. Thompson, T. M. Cronin, S. E. Ishman, and D. A. Willard (1999), Middle Pliocene paleoenvironmental reconstruction; PRISM2, *U.S. Geol. Surv. Open File Rep., 99-535*. (Available at http://pubs.usgs.gov/openfile/of99-535)

Dvorkin, J., A. Nur, G. Mavko, and Z. Ben-Avraham (1993), Narrow subducting slabs and the origin of backarc basins, *Tectonophysics*, *227*, 63–79.

Engdahl, E. R., R. D. van der Hilst, and R. P. Buland (1998), Global teleseismic earthquake relocation with improved travel times and procedures for depth determination, *Bull. Seismol. Soc. Am.*, *88*, 722–743.

Fischer, K. M., and W. R. McCann (1984), Velocity modeling and earthquake relocation in the northeast Caribbean, *Bull. Seismol. Soc. Am.*, *74*, 1249–1262.

Frank, F. C. (1968), Curvature of island arcs, *Nature*, *220*, 363.

Fryer, P., N. Becker, B. Appelgate, F. Martinez, M. Edwards, and G. Fryer (2003), Why is the Challenger Deep so deep?, *Earth Planet. Sci. Lett.*, *211*, 259–269.

Fujioka, K., K. Okino, T. Kanamatsu, and Y. Ohara (2002), Morphology and origin of the Challenger Deep in the southern Mariana Trench, *Geophys. Res. Lett.*, *29*(10), 1372, doi:10.1029/2001GL013595.

Hall, C. E., M. Gurnis, M. Sdrolias, L. L. Lavier, and R. D. Mueller (2003), Catastrophic initiation of subduction following forced convergence across fracture zones, *Earth Planet. Sci. Lett.*, *212*, 15–30.

House, M. A., M. Gurnis, P. J. J. Kamp, and R. Sutherland (2002), Uplift in the Fiordland region, New Zealand: Implications for incipient subduction, *Science*, *297*, 2038–2041.

Gill, I., P. P. McLaughlin Jr., and D. K. Hubbard (1999), Evolution of the Neogene Kingshill Basin of St. Croix, U.S. Virgin Islands, in *Caribbean Basins*, edited by P. Mann, pp. 343–366, Elsevier, New York.

Giunchi, C., R. Sabadini, E. Boschi, and P. Gasperini (1996), Dynamic models of subduction: Geophysical and geological evidence in the Tyrrhenian Sea, *Geophys. J. Int.*, *126*, 555–578.

Gutscher, M. A., J. Malavieille, S. Lallemand, and J. Y. Collot (1999), Tectonic segmentation of the North Andean margin: Impact of the Carnegie Ridge collision, *Earth Planet. Sci. Lett.*, *168*, 255–270.

Gvirtzman, Z., and R. J. Stern (2004), Bathymetry of Mariana trench-arc system and formation of the Challenger Deep as a consequence of weak plate coupling, *Tectonics*, *23*, TC2011, doi:10.1029/2003TC001581.

Isacks, B., L. R. Sykes, and J. Oliver (1969), Focal mechanisms of deep and shallow earthquakes in the Tonga-Kermadec region and the tectonics of island arcs, *Geol. Soc. Am. Bull.*, *80*, 1443–1469.

Jansma, P. E., G. S. Mattioli, A. Lopez, C. DeMets, T. H. Dixon, P. Mann, and E. Calais (2000), Neotectonics of Puerto Rico and the Virgin Islands, northeastern Caribbean, from GPS geodesy, *Tectonics*, *19*, 1021–1037.

Jany, I., K. M. Scanlon, and A. Mauffret (1990), Geological interpretation of combined Seabeam, GLORIA and seismic data from Anegada Passage (Virgin Islands, north Caribbean), *Mar. Geophys. Res.*, *12*, 173–196.

Larue, D. K., R. Torrini Jr., A. L. Smith, J. Joyce, and E. G. Lidiak (1998), North Coast Tertiary basin of Puerto Rico: From arc basin to carbonate platform to arc-massif slope, *Spec. Pap. Geol. Soc. Am.*, *322*, 155–176.

Louie, J. N., S. Chavez-Perez, S. Henrys, and S. Bannister (2002), Multimode migration of scattered and converted waves for the structure of the Hikurangi slab interface, New Zealand, *Tectonophysics*, *355*, 227–246.

Mann, P., E. Calais, J.-C. Ruegg, C. DeMets, P. E. Jansma, and G. S. Mattioli (2002), Oblique collision in the northeastern Caribbean from GPS measurements and geological observations, *Tectonics*, *21*(6), 1057, doi:10.1029/2001TC001304.

Masson, D. G., and K. M. Scanlon (1991), The neotectonic setting of Puerto Rico, *Geol. Soc. Am. Bull.*, *103*, 144–154.

McCann, W. R. (2002), Microearthquake data elucidate details of Caribbean subduction zone, *Seismol. Res. Lett.*, *73*, 25–32.

McCann, W. R., and L. R. Sykes (1984), Subduction of aseismic ridges beneath the Caribbean Plate: Implications for the tectonics and seismic potential of the northeastern Caribbean, *J. Geophys. Res.*, *89*, 4493–4519.

Meyerhoff, A. A., E. A. Krieg, J. D. Cloos, and I. Taner (1983), Petroleum potential of Puerto Rico, *Oil Gas J.*, *81*, 113–120.

Millen, D. W., and M. W. Hamburger (1998), Seismological evidence for tearing of the Pacific Plate at the northern termination of the Tonga subduction zone, *Geology*, *26*, 659–662.

Monroe, W. H. (1980), Geology of the middle Tertiary formations of Puerto Rico, *U.S. Geol. Surv. Prof. Pap.*, *P593*, 93 pp.

Moussa, M. T., G. A. Seiglie, A. A. Meyerhoff, and I. Taner (1987), The Quebradillas Limestone (Miocene-Pliocene), northern Puerto Rico, and tectonics of the northeastern Caribbean margin, *Geol. Soc. Am. Bull.*, *99*, 427–439.

Muszala, S. P., N. R. Grindlay, and R. T. Bird (1999), Three-dimensional Euler deconvolution and tectonic interpretation of marine magnetic anomaly data in the Puerto Rico Trench, *J. Geophys. Res.*, *104*, 29,175–29,187.

Pacheco, J. F., L. R. Sykes, and C. H. Scholz (1993), Nature of seismic coupling along simple plate boundaries of the subduction type, *J. Geophys. Res.*, *98*, 14,133–14,159.

Reid, J. A., P. W. Plumley, and J. H. Schellekens (1991), Paleomagnetic evidence for Late Miocene counterclockwise rotation of north coast carbonate sequence, Puerto Rico, *Geophys. Res. Lett.*, *18*, 565–568.

Robinson, R. (1994), Shallow subduction tectonics and fault interaction: The Weber, New Zealand, earthquake sequence of 1990–1992, *J. Geophys. Res.*, *99*, 9663–9679.

Sandwell, D. T., and W. H. F. Smith (1997), Marine gravity anomaly from Geosat and ERS 1 satellite altimetry, *J. Geophys. Res.*, *102*, 10,039–10,054.

Schlager, W. (1998a), Exposure, drowning and sequence boundaries on carbonate platforms, *Spec. Publ. Int. Assoc. Sedimentol.*, *25*, 3–21.

Schlager, W. (1998b), Scaling of sedimentation rates and drowning of reefs and carbonate platforms, *Geology*, *27*, 183–186.

Smith, W. H. F., and D. T. Sandwell (1997), Global sea floor topography from satellite altimetry and ship depth soundings, *Science*, *277*, 1956–1962.

Speed, R. C., and D. K. Larue (1991), Extension and transtension in the plate boundary zone of the northeastern Caribbean, *Geophys. Res. Lett.*, *18*, 573–576.

Stern, R. J. (2004), Subduction initiation: Spontaneous and induced, *Earth Planet. Sci. Lett.*, *226*, 275–292.

Stern, T. A., and W. E. Holt (1994), Platform subsidence behind an active subduction, *Science*, *368*, 233–236.

Stevenson, D. J., and J. S. Turner (1977), Angle of subduction, *Nature*, *270*, 334–336.

Tanioka, Y., L. Ruff, and K. Satake (1995), The great Kurile earthquake of October 4, 1994, tore the slab, *Geophys. Res. Lett.*, *22*, 1661–1664.

ten Brink, U. S., W. P. Dillon, A. Frankel, R. Rodriguez, and C. Mueller (1999), Seismic and tsunami hazards in Puerto Rico and the Virgin Islands, *U.S. Geol. Surv. Open File Rep.*, *99-353*. (Available at http://pubs.usgs.gov/openfile/of99-353/)

ten Brink, U. S., D. F. Coleman, and W. P. Dillon (2002), The nature of the crust under Cayman Trough from gravity, *Mar. Pet. Geol.*, *19*, 971–987.

ten Brink, U. S., W. W. Danforth, C. Polloni, B. Andrews, P. Llanes, S. V. Smith, E. Parker, and T. Uozumi (2004), New sea floor map of the Puerto Rico trench helps assess earthquake and tsunami hazards, *Eos Trans. AGU*, *85*, 349, 354.

Toda, S., and R. S. Stein (2002), Response of the San Andreas Fault to the 1983 Coalinga-Nunez earthquakes: An application of interaction-based probabilities for Parkfield, *J. Geophys. Res.*, *107*(B6), 2126, doi:10.1029/2001JB000172.

Toth, J., and M. Gurnis (1998), Dynamics of subduction initiation at preexisting fault zones, *J. Geophys. Res.*, *103*, 18,053–18,067.

van Gestel, J.-P., P. Mann, J. F. Dolan, and N. R. Grindlay (1998), Structure and tectonics of the upper Cenozoic Puerto Rico–Virgin Islands carbonate platform as determined from seismic reflection studies, *J. Geophys. Res.*, *103*, 30,505–30,530.

van Gestel, J.-P., P. Mann, N. R. Grindlay, and J. F. Dolan (1999), Three-phase tectonic evolution of the northern margin of Puerto Rico as inferred from an integration of seismic reflection, well, and outcrop data, *Mar. Geol.*, *161*, 259–288.

Vogt, P. R., A. Lowrie, D. R. Bracey, and R. N. Hey (1976), Subduction of aseismic oceanic ridges: Effects on shape, seismicity, and other characteristics of consuming plate boundaries, *Spec. Pap. Geol. Soc. Am.*, *172*, 59 pp.

Watts, A. B. (2001), *Isostasy and Flexure of the Lithosphere*, Cambridge Univ. Press, New York.

Zapp, A. D., H. R. Bergquist, C. R. Thomas, and H. R. Berquist (1948), Tertiary geology of the coastal plains of Puerto Rico, *U.S. Geol. Surv. Oil Gas Invest. Map, OM-0085*, 52–54.

Zhong, S., and M. Gurnis (1992), Viscous flow model of a subduction zone with a faulted lithosphere: Long and short wavelength topography, gravity and geoid, *Geophys. Res. Lett.*, *19*, 1891–1894.

Zhong, S., and M. Gurnis (1994), Controls on trench topography from dynamic models of subducted slabs, *J. Geophys. Res.*, *99*, 15,683–15,695.

U. ten Brink, U.S. Geological Survey, Woods Hole, MA 02543, USA. (utenbrink@usgs.gov)